

1 Assessing PM_{2.5} Exposures with High Spatio-
2 Temporal Resolution across the Continental
3 United States

4 *Qian Di*^{†*}, *Itai Kloog*^{†,‡}, *Petros Koutrakis*[†], *Alexei Lyapustin*[§], *Yujie Wang*[§], *Joel*
5 *Schwartz*[†]

6 [†] Department of Environmental Health, Harvard T.H. Chan School of Public Health,
7 Boston, MA, 02115, USA

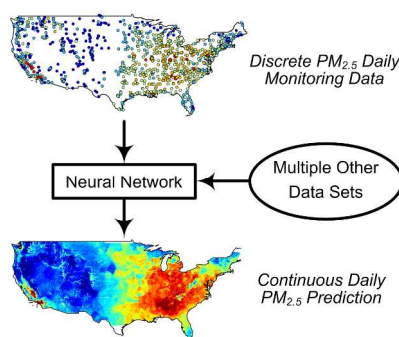
8 [§] GEST/UMBC, NASA Goddard Space Flight Center, Baltimore, MD, USA

9 KEYWORDS. PM_{2.5}; Aerosol optical depth; GEOS-Chem; Absorbing aerosol index;
10 Land-use regression; Convolutional neural network

11

12

13 ABSTRACT. A number of models have been developed to estimate $PM_{2.5}$ exposure,
14 including satellite-based aerosol optical depth (AOD) models, land-use regression or
15 chemical transport model simulation, all with both strengths and weaknesses. Variables
16 like normalized difference vegetation index (NDVI), surface reflectance, absorbing
17 aerosol index and meteoroidal fields, are also informative about $PM_{2.5}$ concentrations.
18 Our objective is to establish a hybrid model which incorporates multiple approaches and
19 input variables to improve model performance. To account for complex atmospheric
20 mechanisms, we used a neural network for its capacity to model nonlinearity and
21 interactions. We used convolutional layers, which aggregate neighboring information,
22 into a neural network to account for spatial and temporal autocorrelation. We trained the
23 neural network for the continental United States from 2000 to 2012 and tested it with left
24 out monitors. Ten-fold cross-validation revealed good model performance with total R^2
25 of 0.84 on the left out monitors. Regional R^2 could be even higher for the Eastern and
26 Central United States. Model performance was still good at low $PM_{2.5}$ concentrations.
27 Then, we used the trained neural network to make daily prediction of $PM_{2.5}$ at $1\text{ km}\times 1$
28 km grid cells. This model allows epidemiologists to access $PM_{2.5}$ exposure in both the
29 short term and the long term.



30

31 1. Introduction

32 Fine particulate matter (PM_{2.5}) is a major concern in public health.¹⁻⁶ Adverse health
33 effect is associated with PM_{2.5} exposure in the short term^{7, 8} and the long term.^{9, 10} PM_{2.5}
34 is found to be associated with morbidity,^{11, 12} mortality,⁶ cardiovascular disease,⁴
35 respiratory disease,¹³ myocardial infarction,¹⁴ an increase in hospital admission^{11, 15, 16}
36 and others.¹⁷

37 Accurate exposure assessment of PM_{2.5} is a prerequisite of to investigate its adverse
38 health effect. Early studies estimated PM_{2.5} at the nearest monitoring station.¹⁸ However,
39 nearest monitors cannot capture all variability in PM_{2.5} concentrations and non-
40 differential misclassification occurs.¹⁹

41 Various approaches have been developed to achieve better exposure assessment.
42 Spatial interpolation, including nearest-neighbor interpolation and Kriging interpolation,
43 was used to smooth PM_{2.5} concentration and estimate local exposure. Nonetheless,
44 interpolation adds no additional information to the model. Local emission like highways
45 between two monitor sites is not captured by simple interpolation. Land-use regression
46 (LUR) uses land-use terms, such as road density, percentage of urban and others, as
47 proxies for PM_{2.5} concentration.^{20, 21} Although LUR could achieve a high spatial
48 resolution, it has limited temporal resolution since land-use terms are usually time-
49 invariant.²² Recent improvements in land-use regression enable to incorporate some level
50 of time-variant factors,^{23, 24} but land-use terms are still inadequate in modeling short-term
51 variations and often limited by short temporal coverage.²⁵

52 Satellite-based aerosol optical depth (AOD) measurements have been widely used to
53 estimate $PM_{2.5}$ in various models for its large spatial coverage and repeated daily
54 observations.²⁶ AOD measures the light extinction due to aerosol in the whole
55 atmospheric column.²⁷ To obtain ground-level $PM_{2.5}$ concentration, vertical distribution
56 of aerosol is needed. Recent studies proposed different calibration methods.^{26, 28-32} Most
57 studies focused on quantifying relationship between AOD and $PM_{2.5}$ or predict long-term
58 average of $PM_{2.5}$, while epidemiological studies also need short-term $PM_{2.5}$ assessment.
59 Some studies combined AOD and land-use regression and used mixed effect model to
60 achieve improvements on model performance.³³⁻³⁵ However, the drawback of AOD is
61 missing data, which is caused by bright surfaces or cloud contamination, especially in
62 winter.³⁶ Also, AOD measurements may also have abnormally large values caused by
63 forest fires.³⁷ For grid cells with missing or abnormal values, the AOD- $PM_{2.5}$ relationship
64 may be problematic, especially for daily $PM_{2.5}$ assessment. The relationship between
65 column aerosol concentration and ground-level concentration can be influenced by
66 multiple factors such as meteorological fields, chemical profile of aerosol and others.^{38, 39}
67 Absorbing aerosol index (AAI) provides information about aerosol type and is
68 informative to $PM_{2.5}$ modeling.^{40, 41}

69 Chemical transport models (CTMs), like GEOS-Chem,⁴² CMAQ,⁴³ and CHIMERE,⁴⁴
70 simulate the formation, dispersion and deposition of fine particles based on emission
71 inventories and known atmospheric chemical reaction. CTM is another way to assess
72 $PM_{2.5}$ concentration. Due to the complexity of reactions and atmospheric meteorological
73 processes, simulated concentration often deviates from the real world. CTM outputs are
74 often used after calibration.^{45, 46} CTM provides aerosol vertical profile, which has been

75 used as scaling factor in AOD calibration.^{29, 47} Due to the limit of computation, CTM
76 usually has coarse spatial resolution. In a previous study, we have proposed a hybrid
77 model which uses land-use regression to downscale CTM outputs.⁴⁸

78 Existing approaches have both strengths and weaknesses and often they complement
79 to each other. In this paper, we incorporated multiple variables into a neural network-
80 based hybrid model, including satellite-based AOD data, AAI, CTM outputs, land-use
81 terms and meteorological variables. We validated the model with ten-fold cross-
82 validation and predicted daily PM_{2.5} at 1 km×1 km resolution in the continental United
83 States for the years 2000-2012. Prediction with such a high temporal and spatial
84 resolution allows epidemiological studies to estimate health effect of PM_{2.5} with greater
85 reliability.

86 **2. Materials**

87 **2.1. Study Domain**

88 The study domain is the continental United States, including 48 contiguous states and
89 Washington D.C (Figure S1). The study period is from January 1st, 2000 to December
90 31st, 2012, in total of 4,749 days.

91 **2.2. Monitoring Data**

92 Monitoring data for PM_{2.5} were collected by EPA Air Quality System (AQS). In total,
93 there were 1,986 monitor stations available in this period and 1,928 of them were located
94 in the study area. Not every monitoring site has data available throughout the study
95 period. Monitoring sites were densely distributed along coastal areas and the Eastern part,

96 while there were few monitors in the Mountain Region (Figure S1). We calibrated our
97 hybrid model to the daily average of monitored PM_{2.5}.

98 **2.3. AOD Data**

99 The Moderate Resolution Imaging Spectroradiometer (MODIS) is an instrument
100 aboard the Earth Observing System (EOS) satellite.^{49, 50} Several algorithms have been
101 developed to retrieve AOD data from MODIS measurement,⁵¹ including a recent
102 algorithm called MAIAC, which retrieves AOD with a spatial resolution of 1 km×1 km.
103 ⁵²⁻⁵⁴ We used MAIAC AOD data from Aqua satellite from 2003 to 2012 and Terra
104 satellite from 2001 to 2012. MAIAC algorithm arranges data at 600 km×600 km tile,
105 which includes 360,000 1 km×1 km grid cells. In total 33 tiles and 11,880,000 grid cells
106 were used in this study, which is also the grid cell we made predictions at. Grid cells over
107 water bodies were excluded from the study.

108 AOD data has some portion of missing values, especially in the winter. Missing
109 values are caused by bright surfaces (e.g. snow coverage) and cloud contamination.³⁶ In
110 addition, AOD data may have abnormally large values due to extreme events like forest
111 fires.³⁷ Usually AOD data with values above 1.5 are excluded from modeling, which also
112 creates missing values.⁵⁵ Our previous study calibrated column aerosol mass from CTM
113 outputs to satellite-based AOD and predicted AOD values when satellite-based AOD are
114 missing.⁵⁶ For AOD data used in this study, we filled in the missing values using this
115 method as pre-processing (Section 3, Supplementary Material).

116 **2.4. Surface Reflectance**

117 Surface characteristics and errors in AOD data products have been well documented
118 by previous studies.⁵⁷ MAIAC algorithm was designed to retrieve AOD over various
119 surfaces, but surface brightness can still affect data quality.⁵⁴ We used MODIS surface
120 reflectance data (MOD09A1) to control for that.⁵⁸ MOD13A1 has a spatial resolution of
121 500 m×500 m and a temporal resolution of 8 days. We used surface reflectance from
122 Band 3 and linearly interpolated values for days without measurements.

123 **2.5. Chemical Transport Model Outputs**

124 We used GEOS-Chem, a chemical transport model, to simulate ground-level PM_{2.5}
125 concentration. GEOS-Chem is a global 3-dimensional chemical transport model, which
126 uses meteorological inputs and emission inventories to simulate atmospheric components.
127 The details of GEOS-Chem is articulated somewhere else.⁴² We performed a nested grid
128 simulation (Version 9.0.2) for North America at 0.500°×0.667° from 2005 to 2012, with
129 boundary conditions exported from a 2.0°×2.5° global simulation. Since meteorological
130 inputs at 0.500°×0.667° are not available from 2000 to 2004, we used 2.0°×2.5° outputs
131 instead. Based on previous studies and pilot testing, total PM_{2.5} was defined as the sum of
132 nitrate, sulfate, elemental carbon, organic carbon, ammonium, sea salt aerosol, dust
133 aerosol and others (Table S2).⁵⁹

134 In addition to providing ground-level PM_{2.5} estimation, GEOS-Chem also simulates
135 vertical distribution of aerosol, which could be used for calibrating AOD. Previous
136 studies used GEOS-Chem to compute the percentage of ground-level aerosol in the total
137 column aerosol. This percentage was used in AOD calibration as a scaling factor.^{29, 60}

138 Both studies utilized GEOS-Chem to provide both direct estimation for ground-level
139 $PM_{2.5}$ and a scaling factor to calibrate AOD.

140 **2.6. Meteorological Data**

141 Meteorological fields were obtained from NCEP North American Regional
142 Reanalysis data, which assimilates various data sources like land-surface, ship,
143 radiosonde, pibal, aircraft, satellite and others.⁶¹ Meteorological data are daily estimate at
144 0.3° grid cells (about 32 km). In total 16 meteorological variables were used in this study.
145 They include air temperature, accumulated total precipitation, downward shortwave
146 radiation flux, accumulated total evaporation, planetary boundary layer height, low cloud
147 area fraction, precipitable water for the entire atmosphere, pressure, specific humidity at
148 2m, visibility, wind speed, medium cloud area fraction, high cloud area fraction, and
149 albedo. Wind speed was computed as the vector sum of u-wind (east-west component of
150 the wind) at 10m and v-wind (north-south component) at 10m.

151 **2.7. Aerosol Index Data**

152 Absorbing aerosol index (AAI) indicates the presence of absorbing aerosols in the
153 atmosphere. Major sources of absorbing aerosol include biomass burning and desert dust;
154 other minor sources could be volcanic ash.⁶² AAI is informative for estimating absorbing
155 aerosols, such as organic carbon and soil dust.^{63, 64} We used AAI Level 3 data products
156 from the Ozone Monitoring Instrument (OMI), where two algorithms are used in
157 retrieval. One is a near-UV algorithm, which retrieves UV aerosol index (OMI data
158 product OMAERUVd);^{62, 64} and the other one uses multi-wavelength aerosol algorithm,
159 whose outputs include aerosol indexes at visible and UV range (OMI data product

160 OMAEROe).⁶⁵ Both algorithms have pros and cons, which have been discussed
161 previously.⁶⁶ Both data products are complementary and thus we used both. OMI AAI
162 data is available after October 2004. OMAERUVd data product has a spatial resolution of
163 1°; OMAEROe data product has a spatial resolution of 0.25°.

164 **2.8. Land-use terms**

165 Land-use terms serve as proxies for emissions and are used to capture variations at a
166 small spatial scale, which may not modeled by GEOS-Chem. The detailed process of
167 obtaining land-terms like elevation, road density, NEI (National Emissions Inventory)
168 emission inventory, population density, percentage of urban, and NDVI has been reported
169 somewhere else.⁶⁷ For vegetation coverage, we used percentage of vegetation from
170 NCEP North American Regional Reanalysis data and MODIS MOD13A2, a NDVI data
171 product.⁶⁸ MOD13A2 has a spatial resolution of 1 km×1 km and a temporal resolution of
172 16 days. We linearly interpolated NDVI values for days without measurements.

173 **2.9. Regional and Monthly Dummy**

174 Previous studies found the relationship between AOD and PM_{2.5} have regional and
175 daily variation due to difference in meteorology and aerosol composition.^{38, 69}
176 Atmospheric mechanism is complex and relationships between other variables could also
177 differ temporally and spatially. To account for that, we put monthly and regional dummy
178 variables. Regional dummy variable comes from major climate types in the United States
179 (Figure S3).⁷⁰ Since AOD-PM_{2.5} relationship can change from day to day, daily dummy
180 variables would be ideal. However, training a neural network with 365 indicator variables

181 in addition to the other variables would be computationally intensive, and we used
182 monthly dummy variables as a compromise.

183 3. Methods

184 We trained a neural network with the above variables to monitor PM_{2.5} from the
185 AQS network. The relationships between input variables and PM_{2.5} could be highly
186 nonlinear with complex interactions. Neural networks have the potential to model any
187 type of nonlinearity.^{71, 72} The details of the neural network, such as its structure and
188 training method were articulated in the supplementary material. All input variables
189 covered the entire study area, but some of them were not available in early years or had
190 higher proportions of missing values. Missing values were especially common in Terra
191 and Aqua AOD data. To deal with the missingness problem and different temporal
192 coverages, we adopted the following steps. We used a calibration method to fill in the
193 missing values in Aqua AOD data from 2003 to 2012 and Terra AOD data from 2001 to
194 2012 based on the association of GEOS-Chem outputs and land-use terms with non-
195 missing AOD.⁵⁶ For the other variables with a low fraction of missing values, we
196 interpolated at grid cells with missing values. Regarding temporal coverage, GEOS-
197 Chem outputs, land-use terms, MODIS outputs, and meteorological variables were
198 available throughout the study period. OMI data, Aqua AOD, and Terra AOD were
199 unavailable in earlier years. For years with one or more unavailable variables, we fitted
200 the model with the remaining available variables.

201 Most previous studies used only *in situ* variables for modeling. However, information
202 from neighboring cell can be informative as well. For example, nearby road density,

203 forest coverage and other land-use variables as well as nearby $\text{PM}_{2.5}$ measurements either
204 influence or correlate with local $\text{PM}_{2.5}$ measurements. They are informative for modeling
205 and can improve model performance. We accounted for spatial correlation by using
206 convolutional layers in the neural network.⁷³ A convolutional layer is computed by
207 applying a convolution kernel on an input layer. Values from neighboring cells are
208 combined through the use of the kernel function. The kernel takes the form a function
209 (e.g. weighted average with Gaussian weights based on distance) that produces a scalar
210 estimate from the multidimensional inputs. A convolution layer aggregates nearby
211 information and can simulate some form of autocorrelation. We included convolutional
212 layers for land-use terms and nearby $\text{PM}_{2.5}$ measurements as additional predictor
213 variables to account for spatial autocorrelation. Multiple convolution layers were
214 incorporated to allow the neural network to model even more complex autocorrelation or
215 possible interaction with other variables (Supplementary material). In addition to nearby
216 grid cells, observations from nearby days for the same grid cell can be also informative.
217 To incorporate this, we first fitted a neural network and obtained an initial prediction for
218 $\text{PM}_{2.5}$. We then computed temporal convolution layers and fitted the neural network
219 again with them (Figure S5).

220 To validate model results and avoid overfitting, we used ten-fold cross-validation, in
221 which all monitoring sites were randomly divided into 10%-90% splits. The model was
222 trained with 90% of data and predicted $\text{PM}_{2.5}$ at the remaining 10%. The same process
223 was repeated for other splits. Assembling predicted $\text{PM}_{2.5}$ at ten 10% testing sets yielded
224 predicted $\text{PM}_{2.5}$ for all the monitors. We computed correlation between predicted $\text{PM}_{2.5}$

225 and monitored $\text{PM}_{2.5}$. Spatial and temporal R^2 s were also calculated. Details of
226 calculating R^2 have been specified in the supplementary material.

227 The trained neural network was then used to make daily $\text{PM}_{2.5}$ predictions for each
228 grid cell (1 km \times 1 km) for each day.

229 All programming was implemented in Matlab (version 2014a, The MathWorks, Inc.).

230 4. Results

231 To determine input variables, we compared models with different combinations of
232 input variables based on cross-validated total R^2 . Model comparison indicated that (1) a
233 hybrid model performed better than any subset models (Figure S6); (2) scaling factor was
234 better to be incorporated as a separate input layer (Figure S7); (3) convolutional layers for
235 land-use variables and predicted $\text{PM}_{2.5}$ both improved model performance (Figures S6,
236 S8). Hence, input variables for the final model were GEOS-Chem outputs, Aqua and
237 Terra AOD, scaling factor, OMI AAs, meteorological variables, NDVI, surface
238 reflectance, land-use terms, convolutional layers and regional/monthly dummy variables.
239 Table 1 presents model performance after conducting ten-fold cross-validation. Total R^2
240 between fitted and monitored $\text{PM}_{2.5}$ ranged from 0.74 to 0.88 and spatial R^2 was from
241 0.78 to 0.88. By season, the model usually performed better in summer, followed by
242 autumn, spring, and winter (Table S3). By region, regions in the Eastern United States
243 had the best model performance, followed by the Central United States. The Pacific and
244 Mountain regions had less satisfying model performance. We also found R^2 remained
245 high before 2008 and dropped after 2010 for sub-regions and the whole study area (Table
246 S4). We will discuss possible reasons later. Region name and division are from U.S.

247 census division (Table S1, Figure S2). In terms of spatial pattern, we found an east-west
248 gradient with model performing better in the Eastern and Central United States but less
249 satisfying in the western coast and the Mountain Region (Figure 1). Besides, some areas
250 in the Mountain Region (e.g. Great Basin and Colorado Plateau) with large variability in
251 elevation and surface type have relative low R^2 all the year round. Even in the Eastern
252 United States, where model performance is high in general, areas along Appalachian
253 Mountains and around Ozark Plateau have less satisfying model performance.

254 Figure 2 shows the spatial distribution of total $PM_{2.5}$ in the study area. The Eastern
255 United States generally had higher $PM_{2.5}$ levels than the Western part. Area around
256 Illinois and Ohio, areas around New York City and Philadelphia, and parts of the
257 Southeastern United States witnessed the heaviest $PM_{2.5}$ pollutions in the study area,
258 especially in summer. The San Joaquin Valley, Salt Lake City and Denver stood out in
259 the Western United States for their high $PM_{2.5}$ levels. Regarding temporal trend, the
260 national average dropped from $9.2 \mu\text{g}/\text{m}^3$ in 2003 to $7.5 \mu\text{g}/\text{m}^3$ 2012 (Figure 3). By
261 regions, the declining trend was predominantly in the Eastern United States, with largest
262 reduction occurring in East South Central Region ($5.8 \mu\text{g}/\text{m}^3$).

263 One additional way to validate our exposure estimates is to see if they can reproduce
264 the spatial autocorrelation in $PM_{2.5}$ concentrations. To do this, we calculated the
265 correlation among all pairs of $PM_{2.5}$ monitors in the EPA network, and plotted them as a
266 function of distance. We compared that to the same plot, but using our predicted $PM_{2.5}$
267 concentrations instead (Figure 4). The results show essential identical trends and
268 substantial overlap between the correlations of actual vs modeled $PM_{2.5}$ with distance.

269 5. Discussion

270 Our hybrid model incorporated existing PM_{2.5} models as well as multiple variables
271 and achieved high out-of-sample R², averaging 0.84 (0.74~0.88 by year) over the study
272 period. The model performed better in some eastern regions, with an average out of
273 sample R² of 0.86~0.89 by region. To our best knowledge, our model performance
274 surpasses existing similar studies. Meanwhile, we predicted PM_{2.5} daily concentrations at
275 nationwide 1 km×1 km grid cells from 2000 to 2012. As discussed below, this level of
276 resolution and coverage is an improvement over current PM_{2.5} models and could be
277 beneficial to epidemiological studies. Epidemiologists could identify long-term and short-
278 term exposure of PM_{2.5} in the whole continental United States at individual level, which
279 helps study adverse health effect of PM_{2.5} with higher accuracy.

280 There are several advantages and innovations in our approach. First of all, our model
281 covered the whole United States with a spatial resolution of 1 km×1 km and a temporal
282 resolution of 1 day and achieved high R². As far as we know, if taking coverage,
283 resolution and model performance into consideration, our model performs better than
284 existing models. As mentioned in the introduction part, most PM_{2.5} modeling work that
285 used AOD data focused on the AOD-PM_{2.5} relationship, instead of making predictions.
286 For studies with similar research goal as ours, some of them have done AOD calibration
287 at global scale, but their estimation was long-term average²⁹ or annual average, with
288 some degree of bias (slope=0.68) and modest R² (R²=0.65).⁴⁷ A previous study calibrated
289 AOD to daily monitored PM_{2.5} in the Northeastern United States using mixed model and
290 achieved R² around 0.725~0.904.³¹ A similar study used the similar method for the

291 Southeastern United States and achieved R^2 around 0.63 to 0.85.³² Compared with both
292 regional models, our hybrid nationwide model performs slightly better in the
293 Northeastern United States and much better in the Southeastern United States (Table S6).
294 One reason is that aerosol formation in the Southeastern United States is affected by
295 biogenic isoprene emission from trees;⁷⁴ while isoprene emission from trees in the
296 Northeastern United States is less of a concern. Secondary organic aerosol that results
297 from isoprene has different absorption than other $PM_{2.5}$ components,⁷⁵ which is not well
298 captured by AOD. AAI provides some information about absorption profile, which helps
299 our hybrid model perform much better in the Southeast and almost the same or a little
300 better in the Northeast.

301 Second, our hybrid model integrated most variables that are known to be informative
302 to $PM_{2.5}$ modeling and improved model performance. This study reminds the importance
303 of hybrid framework and also proposes a possible neural network-based approach to
304 implement that. Atmospheric mechanism is complex and a single variable can only
305 capture an incomplete picture. For example, AOD measures the light extinction due to
306 aerosol in the whole atmosphere column. Different aerosols vary in terms of aerosol
307 absorption, which can affect AOD. More complexly, even the same aerosol type could
308 have various absorptions under different meteorological conditions and emission
309 features.³⁹ This discovery suggests that when modeling $PM_{2.5}$ with AOD data, AAI
310 (proxy for aerosol type), meteorological fields and emission profiles are also necessary.
311 There could be many unknown mechanisms intertwining with other variables. Multiple
312 variables are not redundant but complementary, which can recover the original picture of
313 atmospheric process and improve model performance to the best.

314 Third, we used convolutional layer in neural network for PM_{2.5} modeling, which is an
315 innovation of our study. Primarily used in computer science, convolutional kernel is
316 placed over nearby pixels to produce a convolutional layer. Similarly, we used
317 convolutional layers in exposure assessment to aggregate variable values from nearby
318 grid cells or monitoring sites. Previous studies incorporated nearby information by using
319 nearby monitoring measurements, nearby road density or others, which were all pre-
320 specified. Our hybrid model takes multiple convolutional layers, which stand for various
321 ways of aggregating nearby information, and lets learning algorithm decide their relative
322 importance in the model. This approach is versatile and is able to model different
323 neighboring influences, as well as potential interactions with other variables.

324 Last but not least, we used AOD data with missing values been filled by some
325 calibration model. No further processing is required to deal with missing AOD data,
326 which could have been lengthy and cumbersome in previous studies.

327 For the east-west gradient in model performance (Figure 1), previous studies also
328 reported that correlation between MODIS AOD and ground-measured PM_{2.5} is better in
329 the eastern part but poor in the western part, and they attributed poor model performance
330 to relative low PM_{2.5} level and variability of terrain.^{31,41} This study lends support to both
331 statements. We quantified the relationship between model performance and elevation at
332 each monitoring site and found a negative correlation despite of much noise (Figure S10).
333 Similarly, a positive association exists between PM_{2.5} level and model performance
334 (Figure S10), which implies that the drop of model performance after 2010 is probably
335 caused by substantive reduction in PM_{2.5} level after 2010. This is also the reason why the

336 Mountain region, with low $\text{PM}_{2.5}$ level, has poor model performance. Lower level of
337 $\text{PM}_{2.5}$ means lower signal-to-noise ratio and model performance drops as model
338 uncertainty keeps constant. Besides, the reduction of sulfate is mainly responsible for
339 decreasing $\text{PM}_{2.5}$ level. Sulfate is better modeled in GEOS-Chem than other major
340 components like nitrate and ammonium,⁷⁶ so dropping sulfate causes unsatisfying model
341 performance. For the same reason, we saw less satisfying model performance in
342 California despite of its high $\text{PM}_{2.5}$ level, for the reason that California has high amount
343 of nitrate originated from vehicle exhaust compared with the Eastern United States. This
344 argument suggests that it would be informative to include sulfate in $\text{PM}_{2.5}$ modeling work
345 in the future.

346 Our model performance is still good even at low $\text{PM}_{2.5}$ levels. To prove that, we fitted
347 a spline regression of prediction $\text{PM}_{2.5}$ to measured $\text{PM}_{2.5}$. Linearity between measured
348 and predicted $\text{PM}_{2.5}$ holds when $\text{PM}_{2.5}$ level is below $70 \mu\text{g}/\text{m}^3$ and become less obvious
349 above $80 \mu\text{g}/\text{m}^3$ due to insufficient measurements (Figure 5). Bias at high concentration
350 is less of our concern, since there are few days with $\text{PM}_{2.5}$ level above $80 \mu\text{g}/\text{m}^3$ in the
351 study area. If constraining to monitored $\text{PM}_{2.5}$ below $35 \mu\text{g}/\text{m}^3$, the EPA daily standard
352 for $\text{PM}_{2.5}$, our hybrid model performed even better. Mean R^2 increased to 0.85; slope is
353 close 1; and intercept is close to 0 (Table S5). Good model performance at low $\text{PM}_{2.5}$
354 concentrations enables epidemiologists to estimate the adverse effect of $\text{PM}_{2.5}$ even
355 below EPA daily standard.

356 Figure 2 visualizes the spatial distribution of annual and seasonal average of $\text{PM}_{2.5}$.
357 There is also an east-west gradient of $\text{PM}_{2.5}$ level. The Eastern and Central United States

358 suffered relatively heavy PM_{2.5} pollutions, except Appalachian Mountains, Florida
359 Peninsula, and some remote areas in the Northeast. The Southeastern United States,
360 especially Alabama and Georgia, witnessed high PM_{2.5} level in summer and less
361 noticeably in spring and autumn, which results from isoprene emission from trees.
362 Isoprene emission from trees increases with temperature^{74, 77} and peaks in hot summer.⁷⁸
363 The Western United States had relatively low PM_{2.5} levels, but the San Joaquin Valley,
364 Salt Lake City and Denver stood out for its abnormally high PM_{2.5} level, which was also
365 featured by clear seasonality and high PM_{2.5} level in winter. This is caused by
366 temperature inversion in winter which prevents atmospheric convection and trapped air
367 pollution near surface. For temporal trend, the Eastern and Central United States
368 witnessed a decreasing trend in PM_{2.5} level (Figure 3), which is caused by reduction of
369 sulfur dioxide from power plant emission. For seasonal cycle, PM_{2.5} level peaks in
370 summer in the Eastern and Central United States due to long-term transported sulfate
371 from power plants and isoprene-related organic carbon. The winter peaks are probably
372 caused by increased fuel burning for heat, and local temperature inversion that prevents
373 pollution dispersion.

374 Exposure assessments are essential for epidemiological studies. Traditional method of
375 exposure assessment relies on nearest monitors, which constraints the number of
376 available participants and introduces measurement errors. Besides, monitoring data from
377 some monitors are intermittent. Our PM_{2.5} predictions have temporal resolution of 1 day
378 and spatial resolution of 1 km×1 km, which lifts the above limitations. Besides, our
379 hybrid model performs still well at low concentrations. Linearity between predicted and
380 monitored PM_{2.5} still holds at low concentrations, without any signal of bias (Figure 5).

381 Cross-validated R^2 indicates good fit when daily $PM_{2.5}$ level is below $35 \mu\text{g}/\text{m}^3$ (Table
382 S5), which enable epidemiologists to assess the adverse effect of $PM_{2.5}$ even below EPA
383 standard. In the long term, there is little discrepancy between long-term averages of
384 predicted and monitored $PM_{2.5}$, with difference below $1 \mu\text{g}/\text{m}^3$ (Figure S9).

385 Some limitations remain. Our model requires quite a lot of variables, which limits the
386 application in other countries. This data-intensive approach could be difficult in other
387 regions where public data is sparse. For regions with less data available, we might have
388 to make tradeoff between model performance and resolution. For example, instead of
389 daily prediction $PM_{2.5}$ at $1 \text{ km} \times 1 \text{ km}$, we may model annual average of $PM_{2.5}$ or at coarse
390 spatial resolution. Besides, chemical profile of $PM_{2.5}$ is not available in this framework.
391 Previous epidemiological studies suggest various toxicities of $PM_{2.5}$ chemical
392 components,^{79, 80} which is worthy of further investigation.

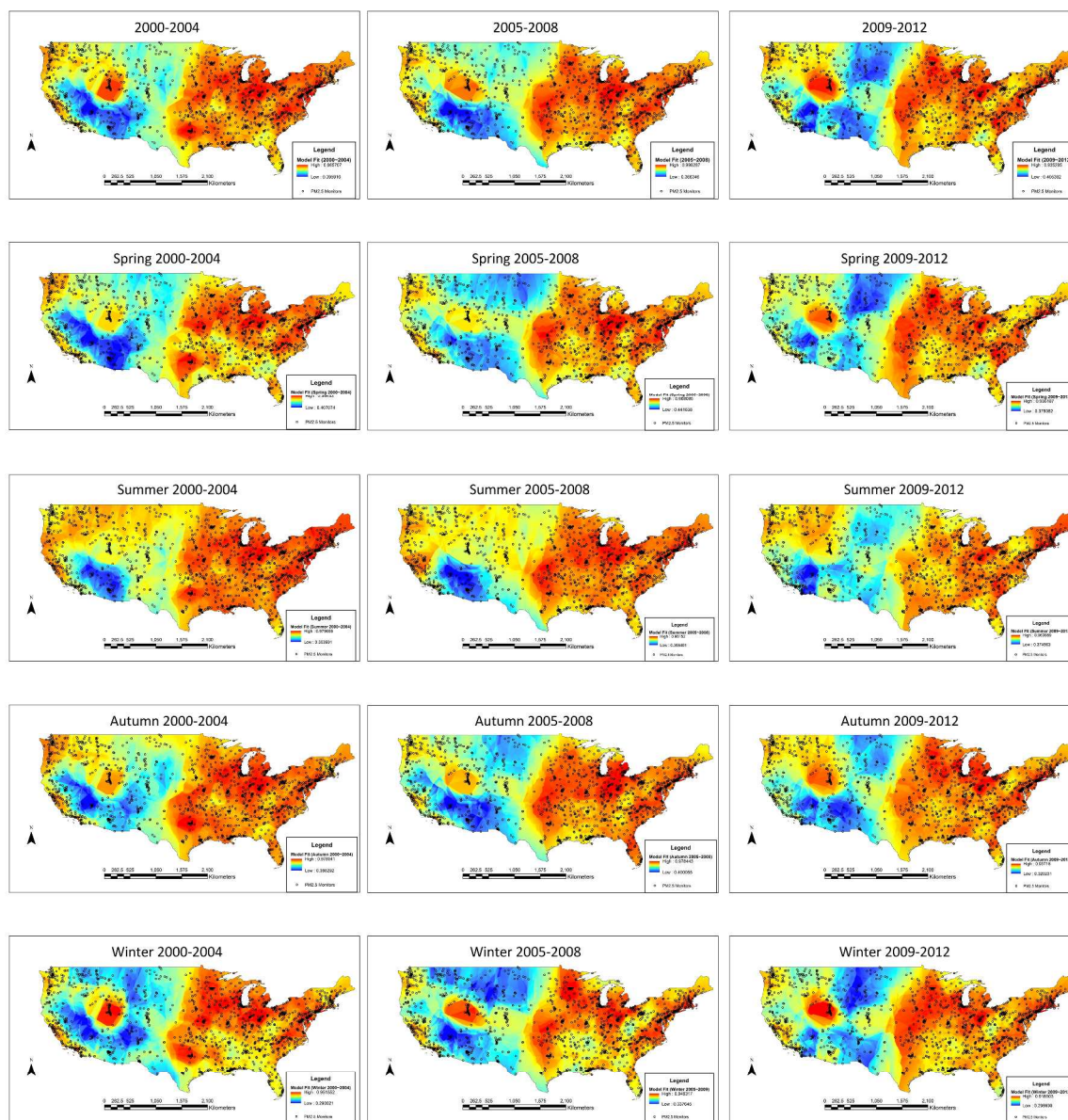
393

394

395 **Table 1. Cross-validated R^2 for the whole study area**

Year	Total R^2	RMSE	Spatial R^2	RMSE	Temporal R^2	RMSE	Bias	Slope
2000	0.86	3.35	0.85	1.52	0.85	3.07	0.22	1.01
2001	0.84	3.58	0.86	1.40	0.83	3.35	0.22	1.01
2002	0.88	2.99	0.88	1.24	0.88	2.75	0.25	1.00
2003	0.88	2.80	0.87	1.21	0.88	2.57	0.23	1.00
2004	0.88	2.69	0.79	1.50	0.88	2.45	0.22	1.00
2005	0.88	2.94	0.84	1.45	0.89	2.66	0.27	1.00
2006	0.86	2.77	0.80	1.34	0.86	2.50	0.25	1.00
2007	0.87	2.95	0.83	1.31	0.87	2.72	0.21	1.00
2008	0.85	2.64	0.79	1.26	0.86	2.40	0.19	1.00
2009	0.82	2.73	0.81	1.09	0.82	2.54	0.21	1.00
2010	0.81	2.85	0.84	1.21	0.81	2.60	0.51	0.98
2011	0.81	2.83	0.81	1.11	0.81	2.60	0.38	0.99
2012	0.74	3.15	0.78	1.16	0.74	2.92	0.32	1.00
Mean	0.84	2.94	0.83	1.29	0.84	2.70	0.27	1.00

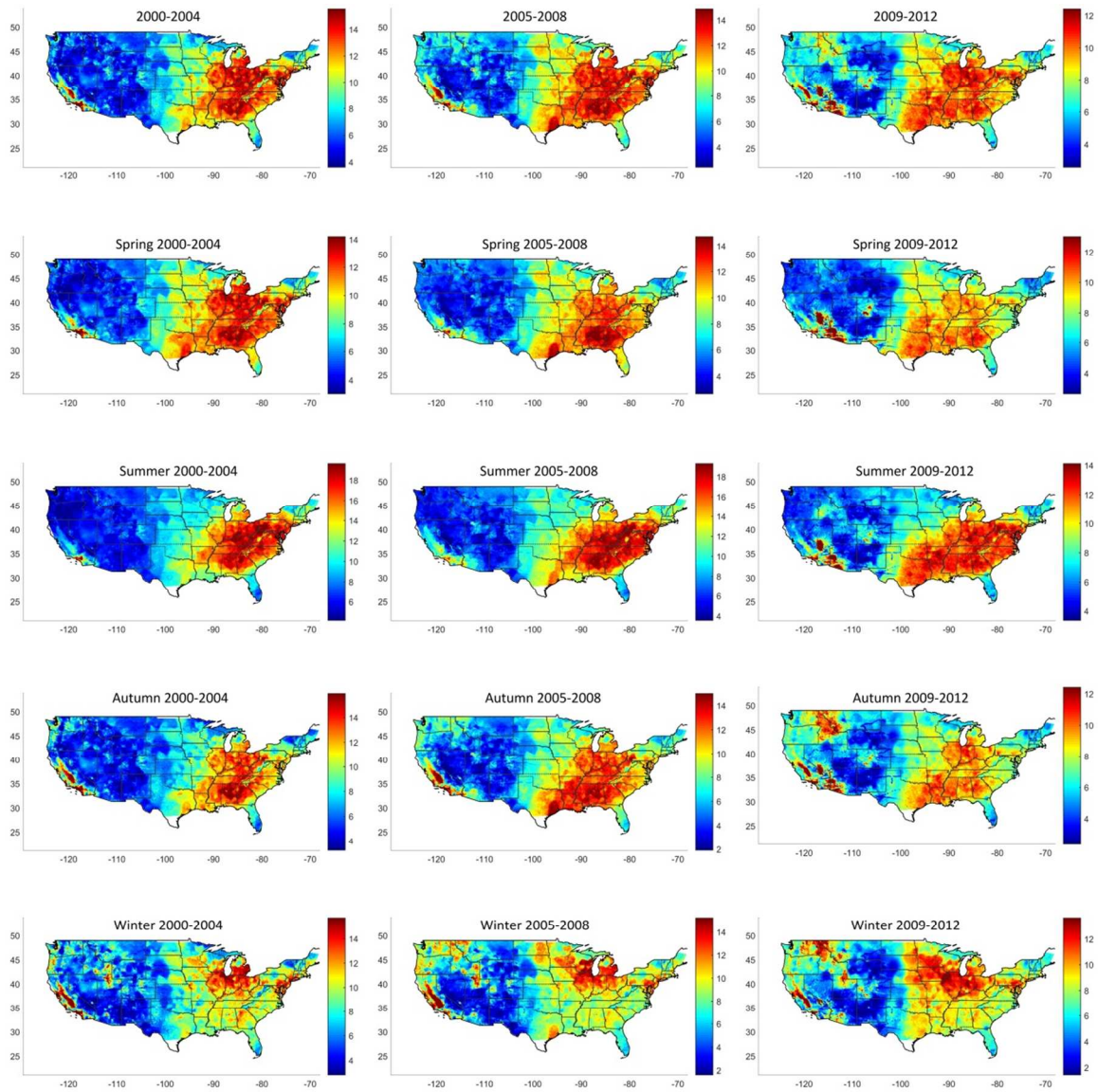
396



397

398 **Figure 1. Model performance in the continental United States**

399 We calculated total R^2 between monitored and predicted $PM_{2.5}$ for each monitoring site
 400 and interpolated R^2 to places without monitors using Kriging interpolation. Spring
 401 defined as March to May; summer was defined as June to August; autumn was defined as
 402 September to November; winter was from December to February of the next year (same
 403 below). Red color stands for high R^2 and blue color stands for low R^2 .

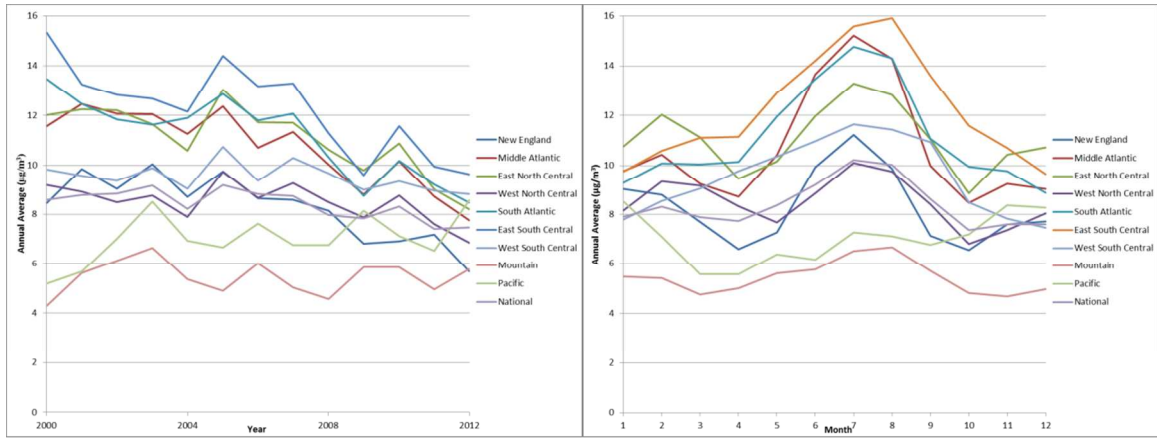


404

405 **Figure 2. Spatial distribution of predicted $PM_{2.5}$**

406 The trained neural network predicted daily total $PM_{2.5}$ concentration at 1 km \times 1 km grid
407 cell in the study area. Red color stands for high concentrations and blue color stands for
408 low concentrations.

409

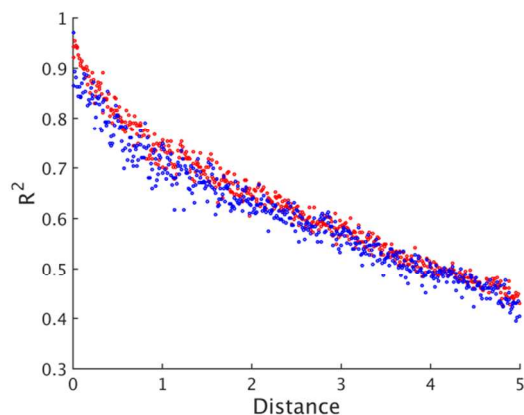


410

411 **Figure 3. Annual means by month of year and by region**412 Annual averages were computed by averaging all predicted PM_{2.5} values at 1 km×1 km

413 grid cells in that region or in that month.

414



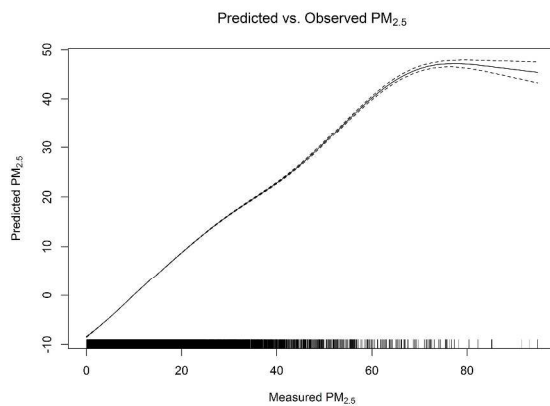
415

416 **Figure 4. Relationship between correlation and distance between any two monitor**
417 **sites**

418 For 1,928 monitoring sites in the study area, we computed the correlation of PM_{2.5}
419 measurements and distance (in degree) between any two monitoring site pairs and plotted
420 the between-site correlation versus between-site distance (red dots). We repeated the
421 same process for predicted PM_{2.5} and plotted the correlation of predicted PM_{2.5} and
422 monitored PM_{2.5} between two site pairs versus distance (blue dots). This figure is for year
423 2012.

424

425



426

427 **Figure 5. Relationship between measured $PM_{2.5}$ and predicted $PM_{2.5}$**

428 We fit a penalized spline between measured $PM_{2.5}$ and predicted $PM_{2.5}$ without

429 specifying degree of freedom. This figure is for year 2009.

430 SUPPORTING INFORMATION

431 Maps of the study area, details on US census division, details on GEOS-Chem, details
432 on neural network and convolutional layers, details on calculating R^2 , detailed results for
433 model comparison, cross-validated R^2 by region and by season, and model performance
434 at low concentrations.

435 AUTHOR INFORMATION

436 **Corresponding Author**

437 *(Q.D.) Phone: 814-777-8202; email: qiandi@mail.harvard.edu

438 **Present Addresses**

439 ‡ Department of Geography and Environmental Development, Ben-Gurion University of
440 the Negev, Beer Sheva, P.O.B. 653, Israel

441 **Author Contributions**

442 The manuscript was written by Qian Di, edited and approved by all authors. All authors
443 have given approval to the final version of the manuscript.

444 ACKNOWLEDGEMENT

445 This publication was made possible by USEPA grant R01 ES024332-01A1,
446 RD83479801, and NIEHS grant ES000002. Its contents are solely the responsibility of
447 the grantee and do not necessarily represent the official views of the USEPA. Further,
448 USEPA do not endorse the purchase of any commercial products or services mentioned
449 in the publication.

450 REFERENCES

- 451 (1). Lim, S. S.; Vos, T.; Flaxman, A. D.; Danaei, G.; Shibuya, K.; Adair-Rohani, H.;
452 AlMazroa, M. A.; Amann, M.; Anderson, H. R.; Andrews, K. G. A comparative risk
453 assessment of burden of disease and injury attributable to 67 risk factors and risk factor
454 clusters in 21 regions, 1990–2010: a systematic analysis for the Global Burden of
455 Disease Study 2010. *The lancet* **2013**, *380*, (9859), 2224-2260.
- 456 (2). Slama, R.; Morgenstern, V.; Cyrus, J.; Zutavern, A.; Herbarth, O.; Wichmann, H.-
457 E.; Heinrich, J.; Group, L. S. Traffic-related atmospheric pollutants levels during
458 pregnancy and offspring's term birth weight: a study relying on a land-use regression
459 exposure model. *Environ. Health Persp.* **2007**, 1283-1292.
- 460 (3). Franklin, M.; Zeka, A.; Schwartz, J. Association between PM_{2.5} and all-cause
461 and specific-cause mortality in 27 US communities. *J. Expo. Sci. Env. Epid.* **2007**, *17*,
462 (3), 279-287.
- 463 (4). Dominici, F.; Peng, R. D.; Bell, M. L.; Pham, L.; McDermott, A.; Zeger, S. L.;
464 Samet, J. M. Fine particulate air pollution and hospital admission for cardiovascular and
465 respiratory diseases. *Jama* **2006**, *295*, (10), 1127-1134.
- 466 (5). Gent, J. F.; Triche, E. W.; Holford, T. R.; Belanger, K.; Bracken, M. B.; Beckett,
467 W. S.; Leaderer, B. P. Association of low-level ozone and fine particles with respiratory
468 symptoms in children with asthma. *Jama* **2003**, *290*, (14), 1859-1867.
- 469 (6). Schwartz, J.; Dockery, D. W.; Neas, L. M. Is daily mortality associated
470 specifically with fine particles? *J. Air Waste Manage. (1995)* **1996**, *46*, 927-939.
- 471 (7). Halonen, J. I.; Lanki, T.; Yli-Tuomi, T.; Kulmala, M.; Tiittanen, P.; Pekkanen, J.
472 Urban air pollution and asthma and COPD hospital emergency room visits. *Thorax*
473 **2008**.
- 474 (8). Zanobetti, A.; Schwartz, J. The effect of fine and coarse particulate air pollution
475 on mortality: a national analysis. *Environ Health Perspect* **2009**, *117*, 898–903.
- 476 (9). Boldo, E.; Medina, S.; Le Tertre, A.; Hurley, F.; Mücke, H.-G.; Ballester, F.;
477 Aguilera, I. Aphis: Health impact assessment of long-term exposure to PM_{2.5} in 23
478 European cities. *Eur. J. Epidemiol.* **2006**, *21*, (6), 449-458.

- 479 (10). Schwartz, J. Harvesting and long term exposure effects in the relation
480 between air pollution and mortality. *Am. J. Epidemiol.* **2000**, *151*, 440-448.
- 481 (11). Lippmann, M.; Ito, K.; Nadas, A.; Burnett, R. Association of particulate
482 matter components with daily mortality and morbidity in urban populations. *Res. Rep.*
483 *HEI* **2000**, (95), 5-72, discussion 73-82.
- 484 (12). Sarnat, J. A.; Marmur, A.; Klein, M.; Kim, E.; Russell, A. G.; Sarnat, S.
485 E.; Mulholland, J. A.; Hopke, P. K.; Tolbert, P. E. Fine particle sources and
486 cardiorespiratory morbidity: an application of chemical mass balance and factor
487 analytical source-apportionment methods. *Environ. Health Persp.* **2008**, *116*, (4), 459.
- 488 (13). Peng, R. D.; Bell, M. L.; Geyh, A. S.; McDermott, A.; Zeger, S. L.;
489 Samet, J. M.; Dominici, F. Emergency Admissions for Cardiovascular and Respiratory
490 Diseases and the Chemical Composition of Fine Particle Air Pollution. *Environ. Health*
491 *Persp.* **2009**, *117*, 957-963.
- 492 (14). Peters, A.; Dockery, D. W.; Muller, J. E.; Mittleman, M. A. Increased
493 Particulate Air Pollution and the Triggering of Myocardial Infarction. *Circulation* **2001**,
494 *103*, 2810-2815.
- 495 (15). Schwartz, J. Air pollution and hospital admissions for cardiovascular
496 disease in Tucson. *Epidemiology* **1997**, 371-377.
- 497 (16). Schwartz, J.; Morris, R. Air pollution and hospital admissions for
498 cardiovascular disease in Detroit, Michigan. *Am. J. Epidemiol.* **1995**, *142*, (1), 23-35.
- 499 (17). Pope, C. A.; Dockery, D. W. Health Effects of Fine Particulate Air
500 Pollution: Lines that Connect. *J. Air Waste Manage.* **2006**, *56*, 709-742.
- 501 (18). Laden, F.; Schwartz, J.; Speizer, F. E.; Dockery, D. W. Reduction in fine
502 particulate air pollution and mortality: extended follow-up of the Harvard Six Cities
503 study. *Am. J. Resp. Crit. Care.* **2006**, *173*, 667-672.
- 504 (19). Pinto, J. P.; Lefohn, A. S.; Shadwick, D. S. Spatial variability of PM_{2.5} in
505 urban areas in the United States. *J. Air Waste Manage.* **2004**, *54*, (4), 440-449.
- 506 (20). Beckerman, B. S.; Jerrett, M.; Martin, R. V.; van Donkelaar, A.; Ross, Z.;
507 Burnett, R. T. Application of the deletion/substitution/addition algorithm to selecting
508 land use regression models for interpolating air pollution measurements in California.
509 *Atmos. Environ.* **2013**, *77*, 172-177.

- 510 (21). Vienneau, D.; De Hoogh, K.; Beelen, R.; Fischer, P.; Hoek, G.; Briggs, D.
511 Comparison of land-use regression models between Great Britain and the Netherlands.
512 *Atmos. Environ.* **2010**, *44*, (5), 688-696.
- 513 (22). Aguilera, I.; Sunyer, J.; Fernández-Patier, R.; Hoek, G.; Aguirre-Alfaro,
514 A.; Meliefste, K.; Bomboi-Mingarro, M. T.; Nieuwenhuijsen, M. J.; Hecce-Garraleta,
515 D.; Brunekreef, B. Estimation of Outdoor NO_x, NO₂, and BTEX Exposure in a Cohort
516 of Pregnant Women Using Land Use Regression Modeling. *Environ. Sci. Technol.* **2008**,
517 *42*, 815-821.
- 518 (23). Ghassoun, Y.; Ruths, M.; Löwner, M.-O.; Weber, S., Intra-urban variation
519 of ultrafine particles as evaluated by process related land use and pollutant driven
520 regression modelling. *Science of the Total Environment* **2015**, *536*, 150-160.
- 521 (24). Patton, A. P.; Zamore, W.; Naumova, E. N.; Levy, J. I.; Brugge, D.;
522 Durant, J. L., Transferability and generalizability of regression models of ultrafine
523 particles in urban neighborhoods in the Boston area. *Environmental science &*
524 *technology* **2015**, *49*, (10), 6051-6060.
- 525 (25). Hoek, G.; Beelen, R.; de Hoogh, K.; Vienneau, D.; Gulliver, J.; Fischer,
526 P.; Briggs, D., A review of land-use regression models to assess spatial variation of
527 outdoor air pollution. *Atmospheric Environment* **2008**, *42*, 7561-7578.
- 528 (26). Streets, D. G.; Canty, T.; Carmichael, G. R.; de Foy, B.; Dickerson, R. R.;
529 Duncan, B. N.; Edwards, D. P.; Haynes, J. A.; Henze, D. K.; Houyoux, M. R. Emissions
530 estimation from satellite retrievals: A review of current capability. *Atmos. Environ.*
531 **2013**, *77*, 1011-1042.
- 532 (27). Morain, S. A.; Budge, A. M. *Environmental Tracking for Public Health*
533 *Surveillance*. CRC Press: 2012.
- 534 (28). Chu, D. A.; Kaufman, Y.; Zibordi, G.; Chern, J.; Mao, J.; Li, C.; Holben,
535 B. Global monitoring of air pollution over land from the Earth Observing System-Terra
536 Moderate Resolution Imaging Spectroradiometer (MODIS). *J. Geophys. Res. Atmos.*
537 (1984–2012) **2003**, *108*, (D21).
- 538 (29). van Donkelaar, A.; Martin, R. V.; Brauer, M.; Kahn, R.; Levy, R.;
539 Verduzco, C.; Villeneuve, P. J. Global Estimates of Ambient Fine Particulate Matter

540 Concentrations from Satellite-Based Aerosol Optical Depth: Development and
541 Application. *Environ. Health Persp.* **2010**, *118*, 847-855.

542 (30). Van Donkelaar, A.; Martin, R. V.; Park, R. J. Estimating ground-level
543 PM_{2.5} using aerosol optical depth determined from satellite remote sensing. *J.*
544 *Geophys. Res. Atmos. (1984–2012)* **2006**, *111*, (D21).

545 (31). Engel-Cox, J. A.; Holloman, C. H.; Coutant, B. W.; Hoff, R. M.
546 Qualitative and quantitative evaluation of MODIS satellite sensor data for regional and
547 urban scale air quality. *Atmos. Environ.* **2004**, *38*, (16), 2495-2509.

548 (32). Wang, J.; Christopher, S. A. Intercomparison between satellite-derived
549 aerosol optical thickness and PM_{2.5} mass: implications for air quality studies. *Geophys.*
550 *Res. Lett.* **2003**, *30*, (21).

551 (33). Kloog, I.; Chudnovsky, A. A.; Just, A. C.; Nordio, F.; Koutrakis, P.;
552 Coull, B. A.; Lyapustin, A.; Wang, Y.; Schwartz, J. A new hybrid spatio-temporal
553 model for estimating daily multi-year PM_{2.5} concentrations across northeastern USA
554 using high resolution aerosol optical depth data. *Atmos. Environ.* **2014**, *95*, 581-590.

555 (34). Kloog, I.; Koutrakis, P.; Coull, B. A.; Lee, H. J.; Schwartz, J. Assessing
556 temporally and spatially resolved PM_{2.5} exposures for epidemiological studies using
557 satellite aerosol optical depth measurements. *Atmos. Environ.* **2011**, *45*, 6267-6275.

558 (35). Lee, M.; Kloog, I.; Chudnovsky, A.; Lyapustin, A.; Wang, Y.; Melly, S.;
559 Coull, B.; Koutrakis, P.; Schwartz, J. Spatiotemporal prediction of fine particulate
560 matter using high-resolution satellite images in the Southeastern US 2003–2011. *J.*
561 *Expo. Sci. Env. Epid.* **2015**.

562 (36). Liu, Y.; Paciorek, C. J.; Koutrakis, P. Estimating Regional Spatial and
563 Temporal Variability of PM_{2.5} Concentrations Using Satellite Data, Meteorology, and
564 Land Use Information. *Environ. Health Persp.* **2009**, *117*, 886-892.

565 (37). Li, F.; Ramanathan, V. Winter to summer monsoon variation of aerosol
566 optical depth over the tropical Indian Ocean. *J. Geophys. Res. Atmos. (1984–2012)*
567 **2002**, *107*, (D16), AAC 2-1-AAC 2-13.

568 (38). Schaap, M.; Apituley, A.; Timmermans, R.; Koelemeijer, R.; Leeuw, G. d.
569 Exploring the relation between aerosol optical depth and PM_{2.5} at Cabauw, the
570 Netherlands. *Atmos. Chem. Phys.* **2009**, *9*, (3), 909-925.

- 571 (39). Dubovik, O.; Holben, B.; Eck, T. F.; Smirnov, A.; Kaufman, Y. J.; King,
572 M. D.; Tanré, D.; Slutsker, I. Variability of absorption and optical properties of key
573 aerosol types observed in worldwide locations. *J. Atmos. Sci.* **2002**, *59*, (3), 590-608.
- 574 (40). Hu, R.-M.; Sokhi, R.; Fisher, B. New algorithms and their application for
575 satellite remote sensing of surface PM_{2.5} and aerosol absorption. *J. Aerosol Sci.* **2009**,
576 *40*, (5), 394-402.
- 577 (41). Al-Saadi, J.; Szykman, J.; Pierce, R. B.; Kittaka, C.; Neil, D.; Chu, D. A.;
578 Remer, L.; Gumley, L.; Prins, E.; Weinstock, L. Improving national air quality forecasts
579 with satellite aerosol observations. *B. Am. Meteorol. Soc.* **2005**, *86*, (9), 1249-1261.
- 580 (42). Bey, I.; Jacob, D. J.; Yantosca, R. M.; Logan, J. A.; Field, B. D.; Fiore, A.
581 M.; Li, Q.; Liu, H. Y.; Mickley, L. J.; Schultz, M. G. Global modeling of tropospheric
582 chemistry with assimilated meteorology: Model description and evaluation. *J. Geophys.*
583 *Res.* **2001**, *106*, 23073.
- 584 (43). Byun, D. W.; Ching, J. *Science algorithms of the EPA Models-3*
585 *community multiscale air quality (CMAQ) modeling system*. United States
586 Environmental Protection Agency: Washington, DC, **1999**.
- 587 (44). Bessagnet, B.; Hodzic, A.; Vautard, R.; Beekmann, M.; Cheinet, S.;
588 Honoré, C.; Liousse, C.; Rouil, L. Aerosol modeling with CHIMERE—preliminary
589 evaluation at the continental scale. *Atmos. Environ.* **2004**, *38*, 2803-2817.
- 590 (45). Jun, M.; Stein, M. L. Statistical comparison of observed and CMAQ
591 modeled daily sulfate levels. *Atmos. Environ.* **2004**, *38*, 4427-4436.
- 592 (46). Cordero, L.; Malakar, N.; Wu, Y.; Gross, B.; Moshary, F.; Ku, M.
593 Assessing satellite based PM_{2.5} estimates against CMAQ model forecasts, *SPIE Remote*
594 *Sensing. Int. Soc. Opt. & Polym.*, **2013**, 8890 (Oct 17th),
- 595 (47). van Donkelaar, A.; Martin, R. V.; Brauer, M.; Boys, B. L. Use of satellite
596 observations for long-term exposure assessment of global concentrations of fine
597 particulate matter. *Environ. Health Persp.* **2015**, *123*, (2), 135.
- 598 (48). Di, Q.; Koutrakis, P.; Schwartz, J. A Hybrid Prediction Model for PM_{2.5}
599 Mass and Components Using a Chemical Transport Model and Land Use Regression.
600 *Atmos. Environ.* **2016**, *131*, 390-399.

- 601 (49). King, M. D.; Kaufman, Y. J.; Menzel, W. P.; Tanre, D. Remote sensing of
602 cloud, aerosol, and water vapor properties from the Moderate Resolution Imaging
603 Spectrometer (MODIS). *IEEE T. Geosci. Remote* **1992**, *30*, (1), 2-27.
- 604 (50). Salomonson, V. V.; Barnes, W.; Maymon, P. W.; Montgomery, H. E.;
605 Ostrow, H. MODIS: Advanced facility instrument for studies of the Earth as a system.
606 *IEEE T. Geosci. Remote* **1989**, *27*, (2), 145-153.
- 607 (51). Remer, L. A.; Kaufman, Y. J.; Tanré, D.; Mattoo, S.; Chu, D. A.; Martins,
608 J. V.; Li, R.-R.; Ichoku, C.; Levy, R. C.; Kleidman, R. G.; et al. The MODIS Aerosol
609 Algorithm, Products, and Validation. *J. Atmos. Sci.* **2005**, *62*, 947-973.
- 610 (52). Chudnovsky, A.; Lyapustin, A.; Wang, Y.; Schwartz, J.; Koutrakis, P.
611 Analyses of high resolution aerosol data from MODIS satellite: a MAIAC retrieval,
612 southern New England, US. *First International Conference on Remote Sensing and*
613 *Geoinformation of the Environment* **2013**, 8795 (Aug 5th).
- 614 (53). Lyapustin, A.; Martonchik, J.; Wang, Y.; Laszlo, I.; Korkin, S. Multiangle
615 implementation of atmospheric correction (MAIAC): 1. Radiative transfer basis and
616 look-up tables. *J. Geophys. Res. Atmos. (1984–2012)* **2011**, *116*, (D3).
- 617 (54). Lyapustin, A.; Wang, Y.; Laszlo, I.; Kahn, R.; Korkin, S.; Remer, L.;
618 Levy, R.; Reid, J. Multiangle implementation of atmospheric correction (MAIAC): 2.
619 Aerosol algorithm. *J. Geophys. Res. Atmos. (1984–2012)* **2011**, *116*, (D3).
- 620 (55). van Donkelaar, A.; Martin, R. V.; Park, R. J. Estimating ground-level
621 PM_{2.5} using aerosol optical depth determined from satellite remote sensing. *J. Geophys.*
622 *Res.* **2006**, *111*.
- 623 (56). Di, Q.; Schwartz, J. Using Chemical Transport Model to Fill in the
624 Missingness of Satellite-Based AOD. *Atmos. Environ.* (In review).
- 625 (57). Drury, E.; Jacob, D. J.; Wang, J.; Spurr, R. J.; Chance, K. Improved
626 algorithm for MODIS satellite retrievals of aerosol optical depths over western North
627 America. *J. Geophys. Res. Atmos. (1984–2012)* **2008**, *113*, (D16).
- 628 (58). Vermote, E. MOD09A1 MODIS/Terra Surface Reflectance 8-Day L3
629 Global 500m SIN Grid V006. *NASA EOSDIS Land Processes DAAC.* **2015**.
- 630 (59). Isakov, V.; Touma, J.; Touma, J.; Khlystov, A.; Sattler, M.; Devanathan,
631 S.; Devanathan, S.; Engel-Cox, J.; Weber, S.; McFarland, M.; et al. Estimating Fine

- 632 Particulate Matter Component Concentrations and Size Distributions Using Satellite-
633 Retrieved Fractional Aerosol Optical Depth: Part 2—A Case Study. *J. Air Waste*
634 *Manage.* **2007**, *57*, 1360-1369.
- 635 (60). Liu, Y. Mapping annual mean ground-level PM_{2.5} concentrations using
636 Multiangle Imaging Spectroradiometer aerosol optical thickness over the contiguous
637 United States. *J. Geophys. Res.* **2004**, *109*.
- 638 (61). Kalnay, E.; Kanamitsu, M.; Kistler, R.; Collins, W.; Deaven, D.; Gandin,
639 L.; Iredell, M.; Saha, S.; White, G.; Woollen, J.; et al. The NCEP/NCAR 40-Year
640 Reanalysis Project. *B. Am. Meteorol. Soc.* **1996**, *77*, 437-471.
- 641 (62). Herman, J.; Bhartia, P.; Torres, O.; Hsu, C.; Seftor, C.; Celarier, E. Global
642 distribution of UV-absorbing aerosols from Nimbus 7/TOMS data. *J. Geophys. Res.*
643 **1997**, *102*, (16), 911-16.
- 644 (63). Tegen, I.; Werner, M.; Harrison, S.; Kohfeld, K. Relative importance of
645 climate and land use in determining present and future global soil dust emission.
646 *Geophys. Res. Lett.* **2004**, *31*, (5).
- 647 (64). Torres, O.; Bhartia, P.; Herman, J.; Ahmad, Z.; Gleason, J. Derivation of
648 aerosol properties from satellite measurements of backscattered ultraviolet radiation:
649 Theoretical basis. *J. Geophys. Res. Atmos. (1984–2012)* **1998**, *103*, (D14), 17099-
650 17110.
- 651 (65). Stein-Zweers, D.; Veefkind, P. OMI/Aura Multi-wavelength Aerosol
652 Optical Depth and Single Scattering Albedo Daily L3 Global 0.25x0.25 deg Lat/Lon
653 Grid, version 003. *NASA Goddard Space Flight Center* **2012**.
- 654 (66). Torres, O.; Tanskanen, A.; Veihelmann, B.; Ahn, C.; Braak, R.; Bhartia,
655 P. K.; Veefkind, P.; Levelt, P. Aerosols and surface UV products from Ozone
656 Monitoring Instrument observations: An overview. *J. Geophys. Res. Atmos. (1984–*
657 *2012)* **2007**, *112*, (D24).
- 658 (67). Kloog, I.; Nordio, F.; Coull, B. A.; Schwartz, J. Incorporating Local Land
659 Use Regression And Satellite Aerosol Optical Depth In A Hybrid Model Of
660 Spatiotemporal PM_{2.5} Exposures In The Mid-Atlantic States. *Environ. Sci. Technol.*
661 **2012**, *46*, 11913-11921.

- 662 (68). Didan, K. MOD13A2 MODIS/Terra Vegetation Indices 16-Day L3 Global
663 1km SIN Grid V006. *NASA EOSDIS Land Processes DAAC* **2015**.
- 664 (69). Lee, H.; Liu, Y.; Coull, B.; Schwartz, J.; Koutrakis, P. A novel calibration
665 approach of MODIS AOD data to predict PM_{2.5} concentrations. *Atmos. Chem. Phys*
666 **2011**, *11*, (15), 7991-8002.
- 667 (70). Kottek, M.; Grieser, J.; Beck, C.; Rudolf, B.; Rubel, F. World map of the
668 Köppen-Geiger climate classification updated. *Meteorol. Z.* **2006**, *15*, (3), 259-263.
- 669 (71). Bishop, C. M. *Neural networks for pattern recognition*. Oxford university
670 press: **1995**.
- 671 (72). Haykin, S.; Network, N. A comprehensive foundation. *Neural Networks*
672 **2004**, *2*, (2004).
- 673 (73). LeCun, Y.; Bengio, Y. Convolutional networks for images, speech, and
674 time series. *The handbook of brain theory and neural networks* **1995**, *3361*, (10).
- 675 (74). Sharkey, T. D.; Wiberley, A. E.; Donohue, A. R. Isoprene emission from
676 plants: why and how. *Ann. Bot.* **2008**, *101*, (1), 5-18.
- 677 (75). Claeys, M.; Graham, B.; Vas, G.; Wang, W.; Vermeylen, R.; Pashynska,
678 V.; Cafmeyer, J.; Guyon, P.; Andreae, M. O.; Artaxo, P. Formation of secondary
679 organic aerosols through photooxidation of isoprene. *Science* **2004**, *303*, (5661), 1173-
680 1176.
- 681 (76). Park, R. J.; Jacob, D. J.; Field, B. D.; Yantosca, R. M.; Chin, M. Natural
682 and transboundary pollution influences on sulfate-nitrate-ammonium aerosols in the
683 United States: Implications for policy. *J. Geophys. Res. Atmos. (1984–2012)* **2004**, *109*,
684 (D15).
- 685 (77). Sharkey, T. D.; Singaas, E. L.; Vanderveer, P. J.; Geron, C. Field
686 measurements of isoprene emission from trees in response to temperature and light. *Tree*
687 *Physiol.* **1996**, *16*, (7), 649-654.
- 688 (78). Geron, C.; Harley, P.; Guenther, A. Isoprene emission capacity for US tree
689 species. *Atmos. Environ.* **2001**, *35*, (19), 3341-3352.
- 690 (79). Franklin, M.; Koutrakis, P.; Schwartz, P. The role of particle composition
691 on the association between PM_{2.5} and mortality. *Epidemiology* **2008**, *19*, (5), 680-9.

692 (80). Dai, L.; Zanutti, A.; Koutrakis, P.; Schwartz, J. D. Associations of fine
693 particulate matter species with mortality in the United States: a multicity time-series
694 analysis. *Environ. Health Persp.* **2014**, *122*, 837.